Visual Abstract

Impact behaviour and fractography of 6061 alloy with trace addition of Sn

Monoj Baruah
Department of Industrial and Production Engineering, Assam Engineering College, Guwahati-13, Assam, India
monoj_baruah@rediffmail.com, http://orcid.org/0000-0002-5517-859X

Anil Borah
Department of Mechanical Engineering, Assam Engineering College, Guwahati-13, Assam, India
anilbassam@rediffmail.com

ABSTRACT. The impact behaviour of 6061 alloy with trace amount of 0, 0.04, and 0.08 wt.% Sn was studied in the as-cast (AC), as-roll (AR) and peak-age roll (PAR) processing state. Additionally, the fracture mechanism was also studied in the AC and PAR state. The experimental investigation revealed that at all processing states, trace addition of Sn improves the impact strength of the 6061 alloy. Compared to the other processing states, the PAR condition contribute most to the impact strength. Fractography analyses showed that the fracture in the alloys occurred primarily by the crack propagation of Al(Fe, Mn)Si particles. The fractures in the AC alloys took place by mixed ductile and brittle mode by larger ductile dimples, cracks and cleavages, while in the PAR alloys was primarily by ductile mode by the smaller dimple fractures.

KEYWORDS. Impact behaviour; Fractography; Trace addition; 6061 alloys

OPEN ACCESS

Citation: Baruah, M., Borah, A., Impact behaviour and fractography of 6061 alloy with trace addition of Sn, Frattura ed Integrità Strutturale, 62 (2022) 126-133.

Received: 28.06.2022
Accepted: 03.08.2022
Online first: 10.08.2022
Published: 01.10.2022

INTRODUCTION

6000 series Al alloys have higher resistance to corrosion, good strength and are light in weight. Hence, these alloy series are widely used in the aerospace and defence applications. The properties of 6000 alloys rely on the quantity, composition and morphology of the Mg_2Si and Fe-rich intermetallic particles. Mg_2Si particle strengthen the 6000 alloys [1], whereas, Fe-rich particles contributes to the hardness, but decrease the ductility [2,3].
Trace addition is an art of introducing a minor amount of alloying elements (0.1 wt.% or less) in aluminium for the improvement in the properties. Alloying elements like Mg and Si in 6000 alloys reduce the dislocation motion through formation of hardening Mg_2Si precipitates, thereby increasing the mechanical strength [4]. Sn in 6000 Al alloys is a potential trace element [5-10]. Sn introduction slows down the natural ageing process of 6000 Al alloys, thus helping in keeping the alloy stable during the transportation period from one place to another [5]. It was also observed that Zinc

addition eliminates the negative effect of Sn addition in the properties of high magnesium content 6000 Al alloy [6]. Sn addition in 6000 alloys had been also shown as a potential accelerating artificial age hardening agent [7-9]. He et. al. [10] also reported a positive effect in the tensile strength of 6000 alloy at lower Sn content of 0.03 wt.%.
The previous studies of 6000 Al alloys with trace Sn are limited to the hardness [5-11] and tensile behaviour [6, 9-10]. It is worth mentioning that the studies on the impact behaviour and fractography of 6000 series aluminium alloys with trace Sn are limited. Hence, in this experimental investigation, the impact behaviour of 6061 Al alloy with trace addition 0, 0.04 and 0.08 wt.% Sn was studied systematically in as-cast (AC), as-roll (AR) and peak-age roll (PAR) states. Moreover, the fractography study of the alloys was also carried out in this experimental investigation.

METHODOLOGY

Casting

A vacuum die melting and casting furnace (Make: SwamEquip) was used for casting the 6061 alloys with 0 (Alloy A), 0.04 (Alloy B) and 0.08 (Alloy C) wt.% Sn. The casting setup is shown in Fig. 1. The 6061 alloy bars and tin (Sn) powder purity 99.9% (Make: Loba), was used for preparation of the investigated alloys. Rectangular shaped mild steel die of dimensions 300×100×15 mm was used for casting the alloys. The casting temperature and vacuum pressure used are 750 °C and 800 mbar [11]. The chemical compositions of the alloys were determined by an optical emission spectrometer (Make: Metal Power & Model: Metavision-1008i^3-V). The chemical compositions of the alloys are presented in Tab. 1. The elements present in the alloys are Mg, Si, Fe, Mn, Cu, Sn and Al. The amount of Mg ranged from 0.89-91 wt.%, Si ranged from 0.35-0.37 wt.%, Fe ranged from 0.25-0.24 wt.%, Mn content was 0.12 wt.% and Cu content was 0.05 wt.% and the balanced amount was Al. The ratio of the solubility of Mg and Si is crucial in the 6061 alloy and is responsible for the mechanical properties of the alloy. Mg and Si can form the intermetallic hardening phase Mg_2Si, which is the main strengthening phase in 6061 alloy.

Alloys	Elements						
	Sn	Mg	Si	Fe	Mn	Cu	Al
A	0	0.89	0.35	0.25	0.12	0.05	Balance
B	0.04	0.88	0.36	0.24	0.12	0.05	Balance
C	0.08	0.91	0.37	0.24	0.12	0.05	Balance

Table 1: Composition (wt.%) of the alloys

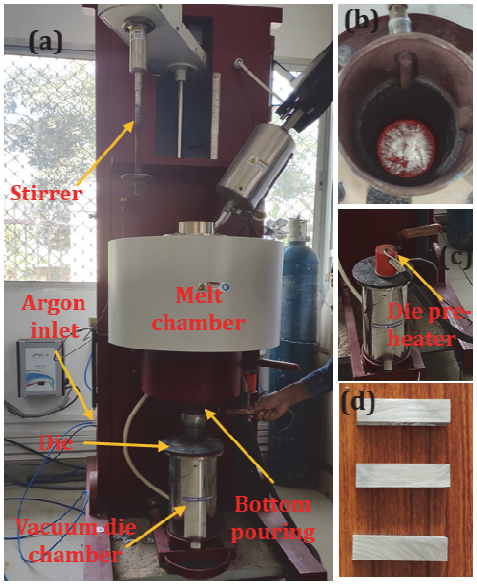

Figure 1: Vacuum-die casting setup (a) Stir melting and casting furnace with vacuum die attachment; (b) Melt chamber; (c) Die pre-heater; (d) Sectioned cast specimens for the preparation of Charpy impact testing.

Processing and heat treatments

After die-casting, the alloys were homogenised for 4 hrs at 530 ℃. The homogenised alloy specimens were then hot rolled at 460 ℃ in a laboratory grade rolling mill (Make: Bharat; Fig. 2). Hot rolling was accomplished in four passes with a total of 28.5% reduction in thickness. The hot rolling temperature of the investigated alloys was based on the data obtained from the literature of Tu et al. [7]. All the hot rolled alloy plates were then peak-aged at 190 ℃ after solution heat treatment for 1 hour at 530 ℃ and quenching in water. The age hardness of the studied alloys was determined by micro-Vickers hardness tester (MVH auto).

Figure 2: Laboratory scale rolling mill.

Impact test

For toughness measurement, Charpy impact tests were conducted on A, B and C alloys in the AC, AR and PAR state, using an impact testing machine (Make: MCS; Model: MIT- 30). Impact testing specimens were prepared from as-cast (AC), as-roll (AR) and peak-age roll (PAR) alloys. The Charpy test specimen (ASTM E23) specifications is shown in Fig. 3.

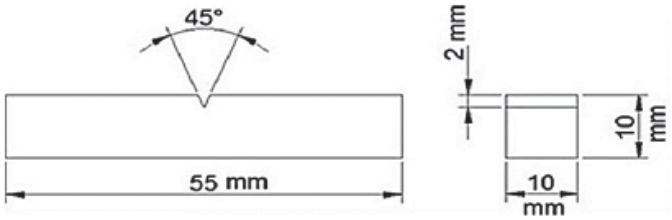

Figure 3: Dimensions of impact test specimen.

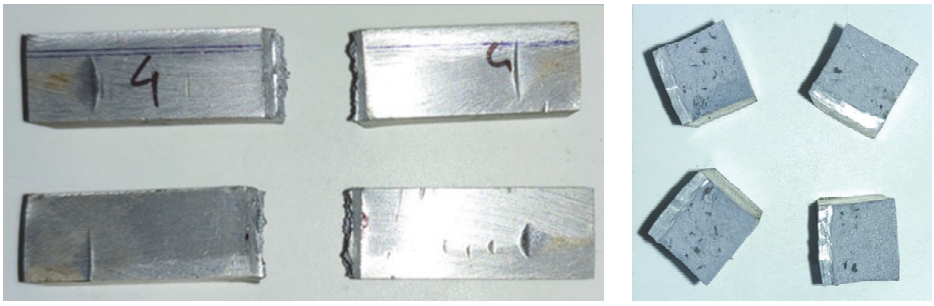

Figure 4: Impact test specimen after fracture.

Fractography

Fig. 4 shows the fracture specimen after the impact test. The impact fracture study of the alloys was carried out in AC and PAR states. Fractography study was carried out using FE-SEM and EDS (Zeiss; Sigma 300).

RESULTS AND DISCUSSIONS

Microstructure

Fig. 5 shows the FE-SEM micrographs of the three alloys in the AC state. The micrograph in Fig. 5 reveals three phases, viz., white (phase A), dark-black (phase B) and light-grey (phase C) in the alloys. From EDS analyses, phase C (light-grey) is identified as Al, phase A (white) is identified as Al(Fe, Mn)Si and phase B (dark-black) is confirmed as Mg_2Si. Detail microstructural studies of the investigated alloys were reported elsewhere [11].

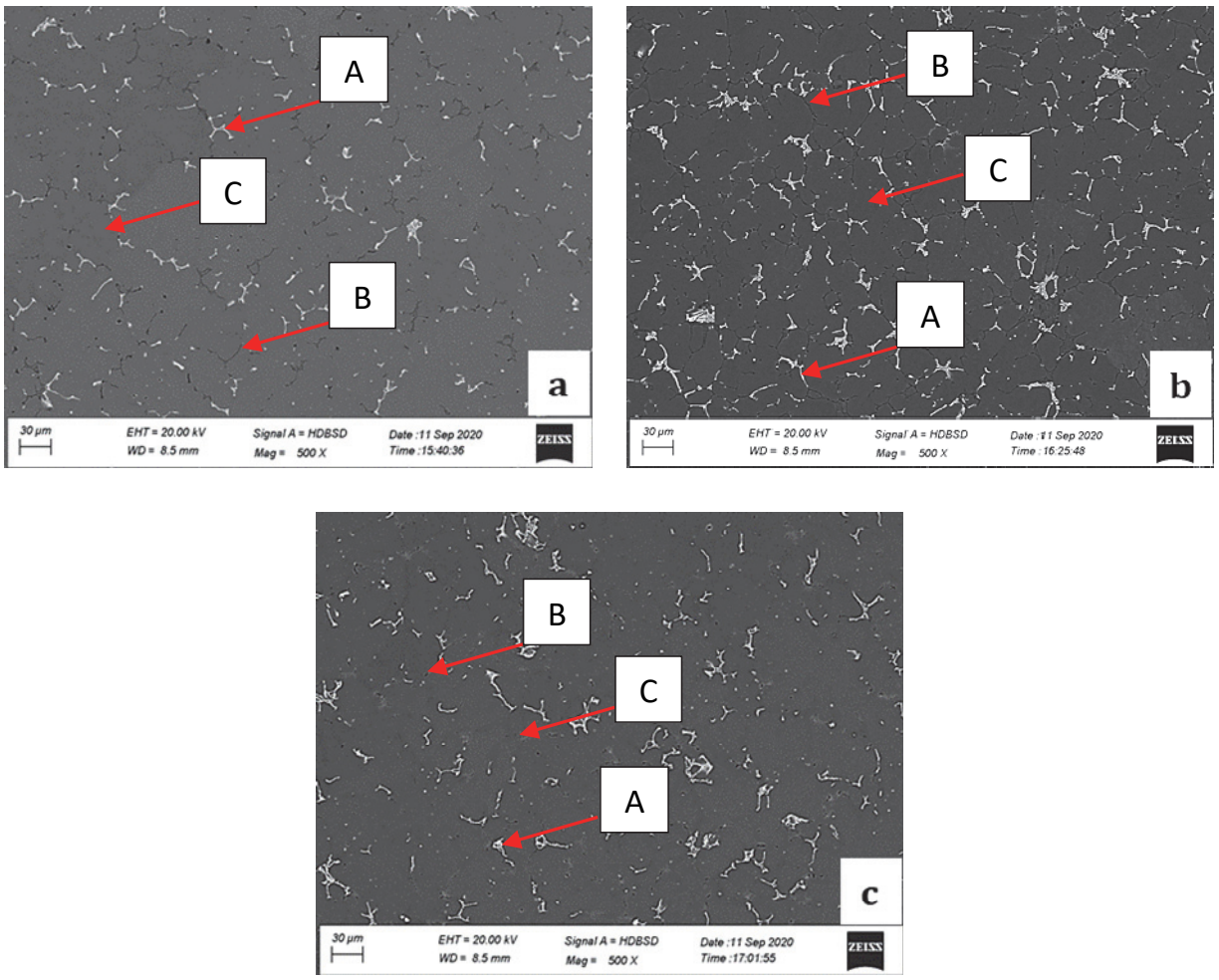

Figure 5: FE-SEM micrographs (a) alloy A, (b) alloy B and (c) alloy C in the as-cast (AC) state.

Ageing

Tab. 2 shows the peak age hardness of the PAR alloys. The peak age hardness of the PAR alloys A, B and C was found as 103, 91 and 114 HV after 12, 6 and 8 hours, respectively. It was found that in comparison to alloy A, the hardness of alloy B decreases and alloy C increases. The decrease and increase in hardness of the alloys with Sn additions is attributed to the increase and decrease in the amount and size of Mg_2Si particles in the matrix and intermetallic phase morphologies [6-11].

Alloys	Peak aged Hardness (HV)	Peak age period (Hours)
A	103	12
B	91	6
C	114	8

Table 2: Peak age hardness of the rolled alloys.

Impact strength

The impact behaviour of the alloys was investigated in AC, AR and PAR state. Fig. 6 shows the impact strengths of the alloys in AC, AR and PAR state. The impact strengths of the A, B and C alloys in AC state were determined as 12, 16 and 22 J, respectively. After hot rolling, the impact strengths of the alloys were increased to 29, 36 and 32 J, and after peak-ageing, impact strengths were further increased to 48, 54 and 53 J, respectively. An increasing trend in the toughness of the alloys was observed from AC state to PAR state. The impact strengths of the AC alloys were increased by 2.4, 2.3 and 1.5 times after hot rolling, and by 4, 3.4 and 2.4 times after peak-ageing treatment, in A, B and C alloys, respectively. It was observed that peak-ageing treatment was more effective in increasing the toughness of the alloys. The marked improvement in the toughness of the alloys after peak-aging can be attributed to the improvement in the ductility [11], as indicated by the finer ductile dimple features on the fracture surface of the alloys in PAR state than AC state (*cf.* Fig. 7). Moreover, it was found that Sn addition had resulted in the increase in impact strength of the 6061 alloys. In the AC state, the highest strength was observed in the alloy C. Whereas, in AR and PAR states, the highest toughness was observed in the alloy B. At maximum strength (i.e., PAR state), the impact strengths 6061 alloy were improved by about 12.5 and 10.4 % by the addition of 0.04 and 0.08 wt.% Sn, respectively.

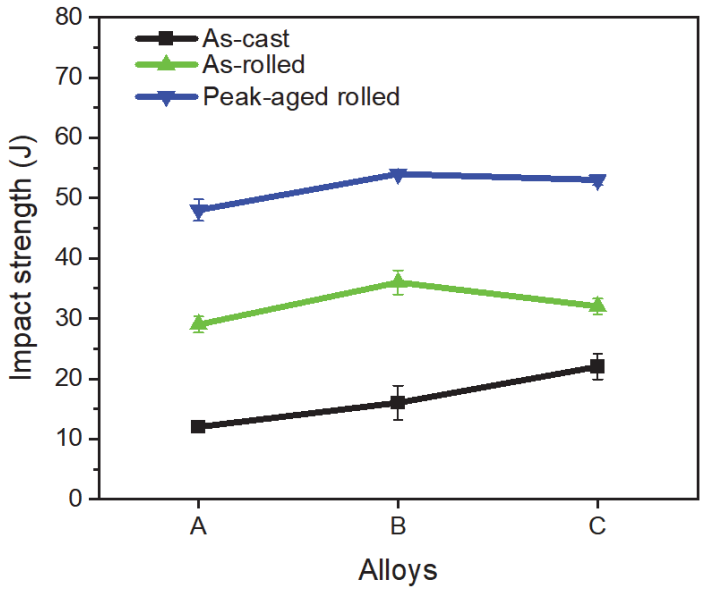

Figure 6: Impact strength of the alloys at various processing stages.

Impact fractography

Fig. 7 shows the impact fracture surfaces of the respective AC and PAR alloy specimens. Fractography of the AC alloys [Figs. 7(a-c)] revealed cracks, facets, and dimples, indicating locally brittle and ductile failure. The Sn-containing as-cast alloys B and C have fewer facets, while these are more prominent in the reference as-cast alloy A. Fractography of the PAR alloys [Figs. 7(d-e)] also revealed cracks, facets, and dimple features. It is observed that dimples are smaller in PAR alloy B than in PAR alloys A and C. A significant difference was also seen in the fracture surfaces of the respective alloys at the AC and the PAR states. It can be seen from Figs. 7(d-f) that relative to AC alloys, the dimples are smaller and denser in PAR alloys. This observation is in line with Xu et al. [13]. The impact fracture surface of the PAR alloys were mostly dominated by smaller dimples, indicating the fracture mechanism is primarily by ductile mode.

Fig. 8 shows the magnified view of the fracture surfaces of the PAR alloys. The presence of second-phase particles in the alloy had resulted in crack propagation, and a larger number of crack particles were observed on the fracture surface. These crack particles are more prominent in the dimple regions. Moreover, coarse dimples could be seen in A and C alloys [*cf.* Figs. 8(a, c)] compared to the fine deep dimples seen in B alloy [*cf.* Fig. 8(b)], which is an indication of better ductility of alloy B [14]. Hence, a higher impact strength can be observed in alloy B in rolled condition. Additionally, from the elemental concentration profile (*cf.* Fig. 8), it could be seen that the concentration of aluminium increases in the tear ridges as compared to the other regions. With the decrease in the intensity of the Al concentration, an increase in the intensity of Mg, Si and Fe concentrations was observed and vice versa. The intensities of the concentration of Si and Fe particles were higher in the fracture surfaces with crack particles than in the fracture surfaces in the absence of the crack particles. The EDS spectrum of the crack particle [see spot 1 in Fig. 8(c)] is also recorded to determine the elemental compositions. The EDS spectrum detects Al, Fe, Mn, Si elements in the crack particles [*cf.* Figs. 8(d)]. This indicates that Al(Fe, Mn)Si elements were accountable for fracture of the alloys [15].

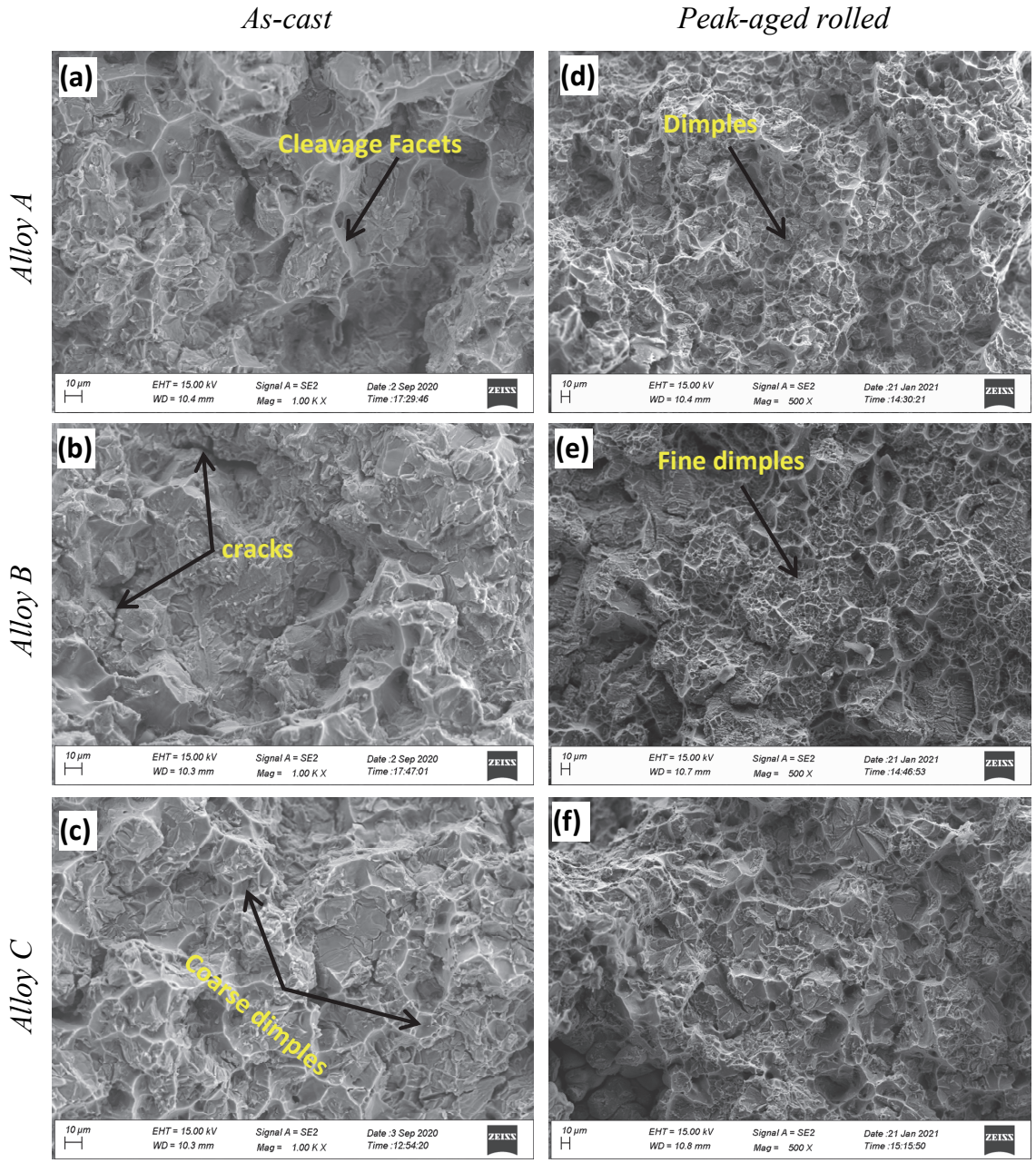

Figure 7: SEM micrograph of impact fracture surface of (a-c) as-cast alloys, (d-f) peak-aged rolled alloys.

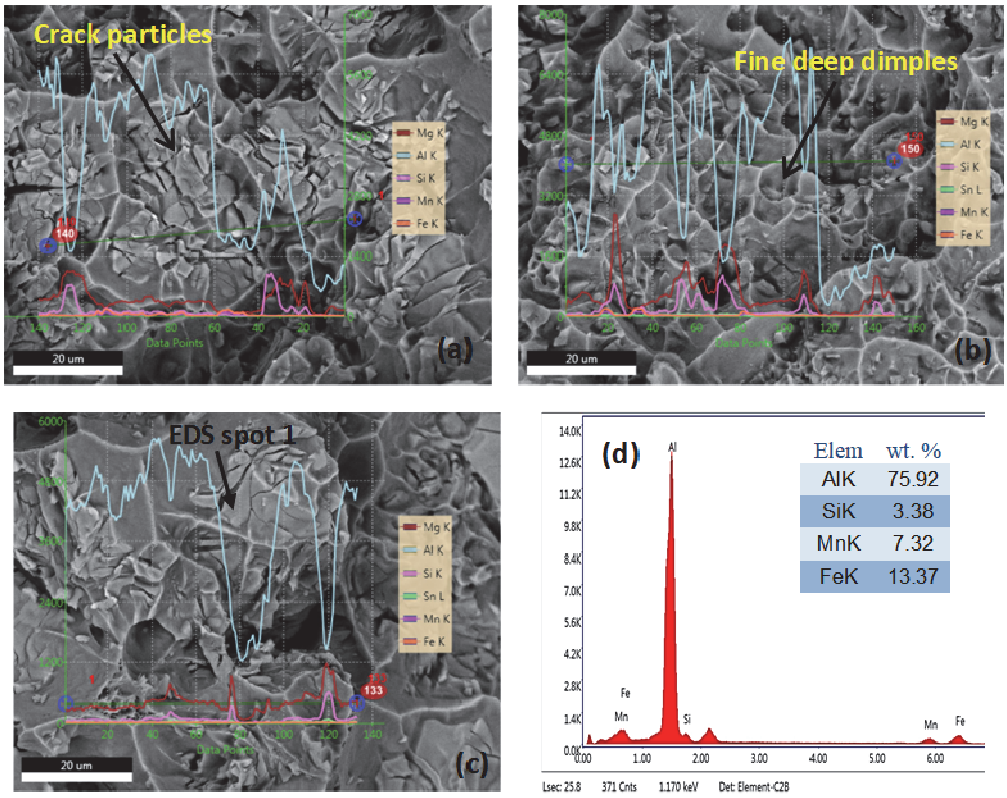

Figure 8: High magnification BSE micrograph of impact fracture surface of peak-aged rolled alloys (a) alloy A (b) alloy B; (c) alloy C and (d) EDS spectrum of spot 1 showing Al(Fe, Mn)Si crack particle.

Conclusions

The impact behaviour and fractography of 6061 alloy with trace additions of 0, 0.04 and 0.08 wt.% Sn were studied, which had not been reported previously under the present set of conditions. The conclusions are summarised as follows: -

1. Trace addition of Sn improves the impact strength of the 6061 alloys is a new finding which has not been reported earlier.
2. The impact strength increases significantly in peak-age roll state.
3. In as-cast state, the maximum impact strength is observed in alloy C with 0.08 wt.% Sn, whereas in as-roll and peak-age roll states the maximum impact strength is observed in alloy B with 0.04 wt.% Sn.
4. The Fe-rich Al(Fe, Mn)Si particles are primarily responsible for fracture of the alloys.
5. The fractures in the as-cast alloys took place by mixed ductile and brittle mode by larger ductile dimples, cracks and cleavages, while, in the peak-age roll alloys was primarily by ductile mode by the smaller dimpled fractures.
6. The enhancement in the impact strength of the alloy due to the addition of Sn may minimise the structural damage of the alloy due to an impact. Hence, one can consider the Sn-added 6061 aluminium alloy suitable for aerospace applications where impact safety is a major concern.

Conflict of Interest

The authors declare that there is no conflict of interests regarding the publication of this paper.

REFERENCES

[1] Mrowka-Nowotnik, G., Sieniawski, J., Wierzbinska M. (2007). Intermetallic phase particles in 6082 aluminium alloy, Archives of Materials Science and Engineering, 28(2), pp. 69-76.

[2] Wang, L., Apelian, D., Makhlouf, M., (1999). Iron-bearing compounds in Al-Si diecasting alloys: Morphology and conditions under which they form, Trans. Am. Found. Soc., 107, pp. 231-238.

[3] Mascre, C. (1955). Fonderie, 108, pp. 4330-4336.

[4] Mrowka-Nowotnik, G., Sieniawski, J., Nowotnik, A. (2009). Effect of heat treatment on tensile and fracture toughness properties of 6082 alloy, Journal of achievements in materials and manufacturing Engineering, 32(2), pp. 1-9.

[5] Werinos, M., Antrekowitsch, H., Ebner, T., Prillhofer, R., Curtin, W.A., Uggowitzer, P.J., Pogatscher, S. (2016). Design strategy for controlled natural aging in Al-Mg-Si alloys, Acta Mater., 118, pp. 296-305. DOI: 10.1016/j.actamat.2016.07.048

[6] Glöckel, F., Uggowitzer, P.J., Felfer, P., Pogatscher, S., Höppel, H.W. (2019). Influence of Zn and Sn on the precipitation behavior of new Al-Mg-Si alloys, Materials, 12(16), pp. 2547. DOI: 10.3390/ma12162547

[7] Tu, W., Tang, J., Zhang, Y., Cao, L., Ma, L., Zhu, Q., Ye, L., Liu, S. (2019). Influence of Sn on the precipitation and hardening response of natural aged Al-0.4Mg-1.0Si alloy artificial aged at different temperatures, Materials Science and Engineering: A., 765, pp. 138250. DOI: 10.1016/j.msea.2019.138250

[8] Zhang, X., Liu, M., Sun, H., Banhart J. (2019). Influence of Sn on the age hardening behavior of Al-Mg-Si alloys at different temperatures, Materialia 8, pp. 100441. DOI:10.1016/j.mtla.2019.100441

[9] Ma, L., Tang, J., Tu, W., Ye, L., Jiang, H., Zhan, X., Zhao, J. (2020). Effect of a trace addition of Sn on the aging behavior of Al-Mg-Si alloy with a different Mg/Si ratio, Materials, 13(4), pp. 913. DOI: 10.3390/ma13040913

[10] He, C., Luo, B., Zheng, Y., Yin, Y., Bai, Z., Ren, Z. (2019). Effect of Sn on microstructure and corrosion behaviours of Al-Mg-Si alloys, Materials Characterization, 156, pp. 109836. DOI: 10.1016/j.matchar.2019.109836

[11] Baruah, M., Borah, A. (2022). Structure–Property Correlation of Al–Mg–Si Alloys Micro-alloyed with Sn, Inter Metalcast., 16, pp. 924–944. DOI: 10.1007/s40962-021-00652-1

[12] Wang, Y., Guo, X., Yang, W., Zhang, J. (2017). Morphology and properties of Mg_2Si and $Mg_2(Si_xSn_1\text{-}x)$ reinforcements in magnesium alloys, Material Science and Technology, 33(15), pp. 1811-1818. DOI: 10.1080/02670836.2017.1322370

[13] Xuehong, X., Deng, Y., Shuiqing, C., Xiaobin, G., (2020). Effect of interrupted ageing treatment on the mechanical properties and intergranular corrosion behavior of Al-Mg-Si alloys, Journal of Materials Research and Technology, 9(1), pp. 230-241. DOI: 10.1016/j.jmrt.2019.10.050

[14] Hui-zhong LI., Ze-xiao ZHU., Xiao-peng LIANG., Peng-wei LI., Ye-long QI., Feng LV., Lan HUANG. (2017). Effect of T6-treatments on microstructure and mechanical properties of forged Al-4.4Cu-0.7Mg-0.6Si alloy, Transactions of Nonferrous Metals Society of China, 27(12), pp. 2539-2547. DOI: 10.1016/S1003-6326(17)60282-6

[15] Kumar, N., Owolabi, G.M., Jayaganthan, R., Goel S. (2018). Correlation of fracture toughness with microstructural features for ultrafine-grained 6082 Al alloy, Fatigue and Fracture of Engineering Materials and Structures, 41(9), pp. 1884-1899. DOI: 10.1111/ffe.12828.